

## **Environmental radioactivity studies in Kabul and northern Afghanistan**

Tanha, M. R.; Ikeda-Ohno, A.; Schulze, M.; Khalid, F. R.; Storai, M. A.; Walther, C.;

Originally published:

October 2018

**Journal of Radioanalytical and Nuclear Chemistry 318(2018)3, 2425-2433**

DOI: <https://doi.org/10.1007/s10967-018-6242-1>

Perma-Link to Publication Repository of HZDR:

<https://www.hzdr.de/publications/Publ-26841>

Release of the secondary publication  
on the basis of the German Copyright Law § 38 Section 4.

## Manuscript Details

<b>Manuscript number</b>	JENVRAD_2018_36
<b>Title</b>	Elevated natural radioactivity in the Kabul area – a radioecological study of rock, soil and drinking water
<b>Article type</b>	Research Paper

### Abstract

From earlier surveys conducted by soviet researchers, the Kabul area was identified as a region of high natural radioactivity. However, only fragmentary maps on dose rates (often only given in relative units) are available. No detailed information of, e.g., uranium and thorium distributions in the upper soil and rock exists. In recent years, residential houses have been built in some of these places known for their elevated radiation dose rate. In order to assess possible radiological risk, 51 soil and rock samples as well as 51 all-purpose water samples were collected and measured with regard to radioisotope content and contamination by other pollutants such as, e.g. heavy metals. For the rocks and soil samples, gamma spectroscopy was used as main technique, while ICP-MS and ICP-OES was used as main technique for water analysis. Furthermore, alpha spectroscopy,  $\mu$ -XRF, PXRD, TOF-SIMS and LSC were used to verify the gamma spectroscopy and ICP-MS results. Activity concentrations in soil and rocks ranged between 160 to 28600 Bq/kg, 73 to 383000Bq/kg, and 270 to 24600 Bq/kg for uranium, thorium, and potassium, respectively. While none of the samples showed any anomalies of the radioactive equilibria some of the samples contained remarkably high levels of thorium and uranium (and their daughter nuclides). Thorium was bound in a cheralite mineral structure. Not all of the investigated waters are safe for drinking, exceeding the national and international recommended values.

**Keywords** Natural radioactivity; elemental concentration; all-purpose water, heavy elements, uranium; thorium; potassium

**Taxonomy** Environmental Monitoring, Environmental Science, Environmental Analysis, Environmental Issues, Environmental Radioactivity

**Corresponding Author** Mohammad R TANHA

**Corresponding Author's Institution** Leibniz Universität Hannover

**Order of Authors** Mohammad R TANHA, Stefan Bister, Elena Laura Mühr-Ebert, Frank Tawussi, Beate Riebe, Stephanie Schneider, Linda Hamann, Alex Hölzer, Atsushi Ikeda-Ohno, Marie schulze, Fazal R Khalid, Mohammad A. Storai, Clemens Walther

**Suggested reviewers** Christian Ekberg, Pavel Povinec

## Submission Files Included in this PDF

### File Name [File Type]

Research highlights.docx [Highlights]

Abstract.docx [Abstract]

Title page.docx [Title Page (with Author Details)]

Manuscript.docx [Manuscript (without Author Details)]

Table.1.docx [Table]

Table.2.docx [Table]

Table.3.docx [Table]

Table.4.docx [Table]

Table.5.docx [Table]

Table.6.docx [Table]

Supplementary information.docx [Supporting File]

## Submission Files Not Included in this PDF

### File Name [File Type]

Fig.1.png [Figure]

Fig.2.png [Figure]

Fig.3a.png [Figure]

Fig.4a.gif [Figure]

Fig.4b.gif [Figure]

Fig.3b.png [Table]

To view all the submission files, including those not included in the PDF, click on the manuscript title on your EVISE Homepage, then click 'Download zip file'.

## Research highlights

- Rock, soil and water from different localities and different sources of Kabul are analyzed
- Alpha and Gamma spectroscopy as well as ICP- MS and ICP- OES, TOF- SIMS, EDX, XRF and XRD is used for analysis
- Some heavy radionuclides and essential nutrients are measured
- The results did not show extreme anomalies, though it does reveal a high level of radioactivity in the area

## Abstract

From earlier surveys conducted by soviet researchers, the Kabul area was identified as a region of high natural radioactivity. However, only fragmentary maps on dose rates (often only given in relative units) are available. No detailed information of, e.g., uranium and thorium distributions in the upper soil and rock exists. In recent years, residential houses have been built in some of these places known for their elevated radiation dose rate. In order to assess possible radiological risk, 51 soil and rock samples as well as 51 all-purpose water samples were collected and measured with regard to radioisotope content and contamination by other pollutants such as, e.g. heavy metals. For the rocks and soil samples, gamma spectroscopy was used as main technique, while ICP-MS and ICP-OES was used as main technique for water analysis. Furthermore, alpha spectroscopy,  $\mu$ -XRF, PXRD, TOF-SIMS and LSC were used to verify the gamma spectroscopy and ICP-MS results. Activity concentrations in soil and rocks ranged between 160 to 28600 Bq/kg, 73 to 383000Bq/kg, and 270 to 24600 Bq/kg for uranium, thorium, and potassium, respectively. While none of the samples showed any anomalies of the radioactive equilibria some of the samples contained remarkably high levels of thorium and uranium (and their daughter nuclides). Thorium was bound in a cheralite mineral structure. Not all of the investigated waters are safe for drinking, exceeding the national and international recommended values.

Title: Elevated natural radioactivity in the Kabul area – a radioecological study of rock, soil and drinking water

Author names and affiliations: Mohammad R. Tanha<sup>1</sup>, Stefan Bister<sup>1</sup>, Elena L. Mühr-Ebert<sup>1</sup>, Frank Tawussi<sup>1</sup>, Beate Riebe<sup>1</sup>, Alex Hölzer<sup>1</sup>, Stephanie Schneider<sup>1</sup>, Linda Hamann<sup>1</sup>, Atsushi Ikeda-Ohno<sup>2</sup>, Marie Schulze<sup>3</sup>, Fazal R. Khalid<sup>4</sup>, Mohammad A. Storai<sup>4</sup> and Clemens Walther<sup>1</sup>

1 - Institute for Radioecology and Radiation Protection, Leibniz Universität Hannover, Hannover, Germany.

2 - Institute of Resource Ecology (IRE) Helmholtz-Zentrum Dresden-Rossendorf (HZDR), Bautzner Landstrasse 400, 01328 Dresden, Germany

3 - Institute for inorganic chemistry, Leibniz Universität Hannover, Hannover, Germany.

4 - Afghan Atomic Energy High Commission, Near Silo-e-Markaz, 1001 Kabul, Afghanistan.

Corresponding author: Mohammad R. Tanha

E-mail: rahmatullahtanha@gmail.com

# Elevated natural radioactivity in the Kabul area – a radioecological study of rock, soil and drinking water

Keywords: Natural radioactivity; elemental concentration; all-purpose water, heavy elements, uranium; thorium; potassium

## Introduction

The level of radioactivity from Naturally Occurring Radioactive Material (NORM) depends on geological conditions and geographical locations [1]. NORM may be present in water, food, soil, rocks, concrete, and other building materials in considerable amounts. The origin of natural radioactivity in rocks and building material is the earth's crust, while the soils' radioactivity often originates from soil minerals. As ground water passes through rocks and soils, it takes up mineral compounds and amongst them radioactive substances due to leaching or alpha recoil [2]. Further sources of radioactivity in nature are technically enhanced natural occurring radioactive material, mineral extraction facilities, extensive use of phosphorus rich fertilizers in agriculture [3], releases from installations of the nuclear fuel cycle, use and tests of nuclear weapons, and fallout from nuclear accidents [4].

As part of a geophysical survey by a Soviet geological survey team conducted in the city and suburbs of Kabul between 1981 and 1985, natural activity levels were measured. Gamma dose rates of up to  $30\mu\text{Sv}/\text{hour}$  were reported using a SANTALIA SONY Pn-68-1 scintillator in the northern parts of Kabul [5]. Since then, residential houses have been built in these areas, while some parts were utilized for rock exploitation, which might have caused health risks for residents and workers [6].

Meanwhile, abnormal isotope ratios between  $^{234}\text{U}$ ,  $^{235}\text{U}$ ,  $^{236}\text{U}$ , and  $^{238}\text{U}$  were reported in urine of Kabul and Nangarhar residents by the Uranium Medical Research Center [7]. In his conclusion, Durakovic claims that his finding predicts the use of CBRN (chemical, biological, radiological, nuclear) weapons. Lack of detailed geological information about the area as well as the loss of existing study files render it difficult to assess, whether the sparse available information is reliable or claims on use of nuclear

weapons in this area can be trusted. Pollutants, and amongst these radioactive material, can enter the environment via the water pathway: Direct discharge of liquid waste into rivers and streams and waste disposal on the land surface are considered the main reason of water pollution in poorly regulated areas. These wastes may contain detergents, food processing waste, fats, and grease, as well as large amounts of chemical pollutants [8]. As one of the fast growing cities in south Asia, Kabul has no well-regulated water supply, sewage and sanitation systems in place. New buildings constructed with foreign aid during the last decade have also been poorly regulated and controlled [9]. Different water sources can contain different variety and levels of radioactivity. Increasing pollution with radioactive contaminants poses health problems to the consumers, thus it is important to determine the concentration of different elements in different sources of drinking water [10]. For daughter radionuclides to be present in large concentrations, the parent radionuclide must be present in the rock material composing the aquifer. However, the occurrence of a parent radionuclide in solution does not necessarily indicate the presence of its decay products due to potentially different geochemical behavior of daughter and the parent element in groundwater [11].

To verify the existing information and claims, the Afghan Atomic Energy High Commission (AAEHC) in collaboration with Afghan Geology Survey (AGS), Afghanistan Urban Water Supply and Sewerage Corporation (AUWSSC) launched a sample collection campaign, which yielded 51 rock and soil samples as well as 51 water samples from Kabul and suburbs. The samples were shipped to the Institute for Radioecology and Radiation Protection (IRS) of the Leibniz Universität Hannover for further analysis.

## Materials and methods

The material and methodology for rock/soil and water samples will be discussed separately here.

## Rocks and Soil sampling locations

One soil and fifty rock samples were collected in three phases between January 2014 and October 2015. In the first phase, one soil and four rock samples were collected from two sampling spots in January and February 2014, in the second phase (October 2014) twenty rock samples were collected from two sampling sites, and in the third phase (October 2015) twenty-six samples were collected from two different sampling sites. The sampling sites are shown in Fig.1.

Fig.1

Authorized reconstructed map from the 1980s, hand drawn by the joint Russian and Afghan survey team. Sampling sites are marked with stars [12].

Due to the presence of residential houses built on the radiation emitting rocks, some of the planned sampling sites could not be accessed. The ambient dose rates of these sites were monitored by a RadEye Personal Radiation Detector (PRD) 100 cm above ground. Rock samples had a weight of about 100 g each. Detailed information on the samples (GPS coordinates, local names, mass, background count rate etc.) are given in table 1 of the supplementary information file.

## Water sampling locations

The study covers an area of about 600 km<sup>2</sup> of Kabul and some of its districts. Attention was paid to collecting the samples from relatively diverse geology in and around Kabul. Samples comprise ground water as well as surface waters, being collected from city water supply taps, kitchen taps, confined and unconfined wells, streams, hand pumps, and bottled water.

Fig.2

Fig.2 Geographical representation of the sampling sites in Kabul (red dots)

The isotopic ratios of different elements were assessed in 51 water samples from different sources. The samples were collected in three different phases between February 2014 and October 2015. In the first phase, most samples were collected from Kabul city water supply network with the help of AUWSSC, while the second and third phases of sampling were performed independently from different locations and

sources. Following AUWSSC's internal procedure and suggestion, the samples collected in the first phase were investigated for zinc, arsenic, nickel, lead, manganese, copper, chromium, barium, aluminum, sodium, magnesium, calcium, and uranium, while in the second and third phase only heavy radionuclides, namely uranium, thorium, and radium were investigated. Samples of 50 mL - 100 mL were collected and bottled in sterilized plastic tubes. The sites were chosen based on availability and diversity of the sources. In the first phase (March 2014) only 8 samples from the city water supply network were collected, in the second phase (October 2014) 23 samples were collected from kitchen taps, confined and unconfined wells, streams, hand pumps, and bottled water. During the third phase in October 2015, 20 samples were collected from kitchen taps, confined and unconfined wells, streams, and hand pumps. After each collection phase, samples were transported to IRS for further investigation. Details about samples sources, locations and conditions is given in supplementary information table 2.

## Gamma ray spectroscopy sample treatment and measurements

Rock and soil samples were collected from the surface with each sampling site covering an area of around 100 m<sup>2</sup>, and were packed in polythene bags. After shipment to IRS, samples were smashed, milled, sealed gas-tight in Marinelli beakers, and stored for one month to attain radioactive equilibrium of the mother and daughter nuclei of the decay chains. All samples were measured by four High Purity Germanium (HPGe) gamma ray spectrometry systems numbered 3, 4, 5, and 6. System number 3 is an Ortec planar detector (42.1% relative efficiency), system number 4 is a Canberra n-type coaxial detector (28.3% relative efficiency), system number 5 is a Canberra n-type planar detector (33.1 % relative efficiency), and system number 6 is a Canberra p-type coaxial detector (35.0 % relative efficiency). The four detector systems have a resolution between 1.76 keV and 1.83 keV for the 1.33MeV photo peak of <sup>60</sup>Co. All detectors are connected to a 16 k multi-channel analyzer (MCA), operated with Maestro II software installed on a DOS operating system for the spectrum analysis. All systems are shielded in order to reduce the influence of background and backscattered radiation. Data were collected in time intervals ranging from 24 to 98 hours for different samples. The energy



range covered 46 - 2000 keV, the efficiency of the detectors was measured using a multi element standard (QCY 48) and a  $^{210}\text{Pb}$  standard sample as reference sources with the same geometry as used for the rock sample measurements. FitzPeaks and QtiPlot software were used for offline analysis of the collected data and fitting of the calibration line distribution, respectively [13, 14]. The most probable peaks which did not appear in the analysis were inserted and fitted manually. The background was measured under comparable conditions and was later subtracted from the measured values.

For a sufficiently old, undisturbed system, all members of the three natural decay chains should be in secular radioactive equilibrium. For a system not in total equilibrium, at least short lived daughter nuclides might be used, as they are fully grown in after approximately five to six half-lives of the daughters [15]. Therefore, for the evaluation of long-lived and non-gamma-emitting daughters, the following gamma lines were picked out. For determination of  $^{238}\text{U}$ , the (1001.03 keV) gamma line of metastable  $^{234\text{m}}\text{Pa}$  was used, while the  $^{214}\text{Pb}$  (295.2 and 352.0 keV) and  $^{214}\text{Bi}$  (1120.29 keV and 1764.49 keV) photo peaks were used for determining  $^{226}\text{Ra}$  as  $^{238}\text{U}$  progeny. To determine  $^{228}\text{Ra}$  as a  $^{232}\text{Th}$  progeny, the  $^{228}\text{Ac}$  (911.20 keV and 968.97 keV) photo peaks were used, while the  $^{212}\text{Pb}$  (238.6 keV) and  $^{208}\text{Tl}$  (583.1 and 860.56 keV) photo peaks were chosen for the  $^{228}\text{Th}$  determination. For  $^{235}\text{U}$  determination, the (163.33 keV and 205.31 keV) photo peaks were used, while the  $^{219}\text{Rn}$  (401.81 keV) and  $^{211}\text{Pb}$  (404.85 keV) photo peaks were picked for determination of  $^{227}\text{Ac}$ . Finally, the 1460.83 keV gamma line was chosen to determine the  $^{40}\text{K}$  activity concentration.

The abundance of a gamma line of a particular energy, which might lead to disturbance of a peak, was taken from literature and the selection was made based on that. Nuclide identification was performed using the FitzPeaks open source gamma energies analytical software. For a better accuracy, energy lines below 100 keV were not included in calculations. Gamma line selection was based on energy line abundance of the concerning isotope and least disturbed peaks of the daughter nuclides:

$^{234\text{m}}\text{Pa}$  emits gamma radiation of 766.37 keV and 1001.03 keV, respectively, where the emission probability of the 1001.03 keV gamma line is higher

than that of the 766.37 keV (0.8% and 0.2% for 1001.03keV and 766.37 keV, respectively). The 766.37 keV line is potentially disturbed by  $^{211}\text{Pb}$  with an energy line of 766.51 keV and an emission probability of 0.3%. Therefore, only the 1001.03 keV line was chosen for determination of  $^{238}\text{U}$ . Even though the line at 185.72 keV is the most probable gamma line of  $^{235}\text{U}$ , the  $^{226}\text{Ra}$  186.1 keV line increases uncertainty for its determination.

During activity calculation, the background counts were subtracted from the gross counts and the following formula was used to calculate the specific activity [16]:

$$a = \frac{k_s}{m\varepsilon\rho_\gamma} * r_n = \omega * r_n \quad 1$$

Where  $a$  is specific activity of the element,  $k_s$  is a nuclide dependent dimensionless correction factor,  $r_n$  is the net count,  $m$  is the mass of the material,  $\varepsilon$  is the efficiency,  $\rho_\gamma$  is the emission probability of a certain isotope and  $\omega$  is the calibration factor.

The uncertainty of the activity is calculated using the following formula [17]:

$$u(a) = \sqrt{r_n^2 * u^2(\omega) + \omega^2 * u^2(r_n)} = \sqrt{a^2 * u_{rel}^2(\omega) + \omega^2 * u^2(r_n)}$$

Where the relative uncertainty  $u_{rel}(\omega)$  is:

$$u_{rel}^2(\omega) = u_{rel}^2(k_s) + u_{rel}^2(m) + u_{rel}^2(\varepsilon) + u_{rel}^2(\rho_\gamma)$$

In order to verify the gamma spectroscopy results, four different methods were used to measure the uranium and thorium concentrations,  $^{238}\text{U}/^{235}\text{U}$  activity ratios as well as identify the mineralogical structure in some samples.

## Alpha spectroscopy sample treatment and measurement

To measure the uranium and thorium isotopes by alpha-spectrometry, one soil and seven rock samples (F1R4, F1S, F2R1, F2R2, F2R9, F3R1, F3R4 and F3R20) have been investigated, where F, R and S denominates phase, rock and soil respectively. The beforehand powdered rock and soil samples were digested by microwave pressure digestion with nitric and hydrofluoric acid at a maximum temperature of 220 °C and a maximum pressure of 120 bar. Uranium and thorium were separated by solid-phase extraction

using UTEVA-cartridges [18]. Following the established separation procedure [19], uranium and thorium were electrodeposited separately onto stainless steel planchets using the method described in the Eichrom working instruction [20]. Alpha-spectrometry measurements of the samples were performed using a Model 7200 Alpha Analyst Integrated Alpha Spectrometer equipped with PIPS-detectors.

### TOF-SIMS sample treatment and measurement

A small amount of the powdered soil sample from the first phase of sampling was pressed on a thin indium foil and covered with an alpha track detector (CN-85, Kodak). After 33 days of exposure, the detector was etched with 10% NaOH at 60°C for 20 min and rinsed with distilled H<sub>2</sub>O. The analysis of the detector with an optical microscope (Eclipse LV-DAF, Nikon) shows a very high amount of heterogeneously distributed spots produced by alpha radiation emitting particles.

A part of the sample, on which many particles were located, was cut out and analyzed with a Time-of-Flight Secondary Ion Mass Spectrometer (TOF-SIMS 5, ION-TOF GmbH, software Surface Lab 6.5). This device scans sample surfaces with primary bismuth ions with 30kV acceleration voltage.

### μ-XRF sample treatment and measurement

To obtain qualitative and semi-quantitative information, a total of 15 samples (sample number 1 to 5 from each of the three sampling phases) were analyzed using Micro X-ray Fluorescence spectroscopy (μ-XRF). An Eagle μ-Probe II (EDAX, Software: Eday-Vision32, Version 3.999) with Rh-target and Si (Li)-detector was used, adjusted to a spot diameter of 50 μm, 40 keV voltage, and vacuum conditions for all analyses. The beforehand prepared sample carriers were fixed in the sample chamber using adhesive tape in order to prevent displacement during analysis. Three spot measurements were performed for each sample using 210-370 mA current, 100 sec measurement time, and 17 μs amplifier shaping time. The quantification was based on a fundamental parameter model (FundParam-Version 35), normalizing the quantified elements to 100 %. Additionally, for two samples elemental mappings

were generated by μ-XRF to locate uraniferous particles (current: 230-320 mA; amplitude time: 10 μs; matrix: 64x50; 128x100; measurement time per spot: 2000 ms, 5000 ms; spot distance: 42-73 μm). Sixteen elements were mapped simultaneously (MgK, AlK, SiK, RhL, PdL, K, CaK, TiK, CrK, MnK, FeK, CoK, CuK, RaL, ThL, U L).

### PXRD sample treatment and measurement

Based on μ-XRF information, a total of 15 samples (sample number 1 to 5 from each of the three sampling phases) were analyzed by powder X-ray diffraction (PXRD) to identify the mineralogical composition of the samples. The measurements were performed using a Rigaku MiniFlex 600 diffractometer equipped with a Cu Kα radiation ( $\lambda = 1.54056 \text{ \AA}$ , 40 kV / 15 mA operation) X-ray source and a D/Tex Ultra Si strip detector with a standard detection mode.

The samples were grinded prior to the measurements, and the samples (approximately 100 mg) were placed on a zero-background Si sample holder of 10.0 mm diameter and 0.2 mm depth. In order to minimize the effect of “preferred orientation” on the acquired diffractograms, the sample holder was constantly rotated horizontally during the measurement. The samples were analyzed under ambient conditions, diffractograms were recorded from 5° to 80° with 0.02° step size.

Acquired PXRD data were analyzed (e.g. background subtraction, peak deconvolution, etc.) with the software PDXL 2 (Version 2.6.1.2) from Rigaku. Based on the elemental information from μ-XRF measurements, phase identification analysis was carried out using the same software combined with the database PDF-4+ 2016 (ICDD).

### SEM-EDX sample treatment and measurement

A pre-powdered homogenous soil sample was fixed on the sample holder using carbon tape, introduced into the instrument and the instrument was evacuated. First, the BSE image was taken to identify the heavy element holding particles. Then a rectangular area of the particle in the sample was measured with the EDX and the graph was evaluated with the help of the software. The image and the graph was taken by a Philips XL30 ESEM with a field emission electron source and a

silicon drift detector for EDX. The operational voltage was set to 25 kV.

## Sample treatment and measurements of the water samples

The water samples were analyzed by the methods described in the previous section applicable to liquid samples. The present section only summarizes treatment, techniques/ instruments and operation parameters different from the ones described above. Gamma spectroscopy was performed using the HPGe (high purity germanium) detectors number 4, 5 and 6. Data were taken in time intervals ranging from 24 to 98 hours for different water samples. The empty bottles were also measured with the identical setup and time interval for acquisition of the background count rate, which was then subtracted from the gross count rate of the samples. The detector energy efficiency was calibrated using a mixed radionuclide standard QCY 48 [21] and  $^{210}\text{Pb}$  as a reference source with the same method used for sample measurements and 82000 sec of live time. FitzPeaks and QtipPlot software were used for offline analysis of the collected data and for fitting the calibration line distribution, respectively. Peaks with high emission probability, which did not appear in the analysis were inserted and refitted.

The water samples of the first sampling phase were measured by gamma spectroscopy without pretreatment. No activity exceeding detection limit was observed. In the next step, ICP-OES and ICP-MS systems were utilized for element identification. Samples were rebottled in 50 ml plastic beakers; a multi standard calibration method with different dilution factors for better accuracy was performed. Zn, As, Ni, Pb, Mn, Cu, Cr, Ba, Al, and U were measured by ICP-MS, whereas Na, Ca, Fe, K, and Pb were measured by ICP-OES.

Uranium, thorium, lead, and radium were measured by ICP-MS with detection limits of 2, 1, 5, and 1 ppt, respectively [22].

In the second phase, 23 water samples from different areas of Kabul were investigated for U, Ra, Th and Pb. Measurements of all samples were carried out by ICP-MS. Due to the potentially enhanced pollutant concentrations, samples were filtered prior to the measurements, rebottled in 50 mL plastic cylinders, and a multi standard calibration was performed.

Standards were prepared with nitric acid with a concentration of 2%. If necessary, samples were diluted with Milli-Q water to match the calibration range.

The samples of the third phase were measured with focus on heavy radionuclides namely U, Ra, Th and Pb using the same ICP-MS device. As in phase two, all samples were filtered and diluted if necessary. Samples number 1, 2, 3, 4, 5, 6, 19, 20, 21, 22 and 23 were additionally measured by LSC alpha spectroscopy in order to confirm the absence of radium in the samples.

## Results and discussions

As in the previous section, the results of a) rock/soil and b) water will be discussed separately, followed by a joint discussion.

### Rocks and soil samples

As far as the geology of the sampling area is concerned, veins of magmatic granite are reported for the Kabul geological block [23]. A comparative study reports significant amounts of granite gneisses containing radioactive elements in the mountains surrounding Kabul [24]. Additionally, Afghanistan is reported as promising exploration area for uranium due to being member of a series of granitic rock orogenic belts [25]. Furthermore, thorium bearing monazite minerals are reported for Kabul surrounding hills [26]. Similarly, an unusually high natural radioactivity originating from enhanced concentrations of thorium in monazite minerals are reported for some beach sands in India, Iran, Brazil, and China [27].

### Gamma Spectroscopy

Considerable amounts of  $^{238}\text{U}$ ,  $^{235}\text{U}$  and  $^{232}\text{Th}$  were detected in samples from the first and second phase, whereas in those of the third phase only one  $^{238}\text{U}$  series daughter, namely  $^{226}\text{Ra}$ , was detected. Signals from all isotopes of the  $^{238}\text{U}$  and  $^{235}\text{U}$  series were lower than the detection limit. A combined average activity concentration of all three phases is shown in Figure 4 of the supplementary information.

The maximum and minimum activity concentrations of all three phases are shown in Table 1.

Table 1

Table 1 displays higher activity concentrations of  $^{238}\text{U}$  and its progenies,  $^{235}\text{U}$  progenies, and  $^{232}\text{Th}$  progenies in our samples as compared to concentrations reported in rocks and soils of most other places of the world [28, 29]

The activity ratio of  $^{238}\text{U}/^{235}\text{U}$  ranges between 1 and 40, which is different from the value of 21.7 discussed in literature for undisturbed natural uranium [30]. Should this value be true, it would strongly suggest admixture of enriched uranium. While depleted uranium admixture would have been plausible from the use of DUA by Soviet troops during the war, the presence of enriched uranium is not easily explained. Hence additional investigations were performed.

### Alpha spectroscopy

All investigated samples show a clear excess of thorium over uranium-with the thorium activity being 1.7 to 20.5 times higher than the uranium activities. On average, the thorium activity is 8.7 times that of the uranium activity. Alpha spectrometry results do not indicate the presence of artificial or abnormal uranium isotope composition, and both isotope ratios of  $^{234}\text{U}/^{238}\text{U}$  and  $^{235}\text{U}/^{238}\text{U}$ , respectively, are consistent with the natural isotope composition of uranium.

The majority of the samples show compliant activities for  $^{238}\text{U}$  and  $^{230}\text{Th}$ , confirming the expected secular equilibrium. Those samples showing considerable deviations from the equilibrium in both directions might probably be influenced by surficial weathering of the rocks. [31, 32]

### TOF-SIMS

First analyses by TOF-SIMS showed a high amount of thorium and uranium containing particles distributed on an area of  $500 \times 500 \mu\text{m}$ . One of these particles was analyzed with a special mode for high quality secondary ion images. These images are presented in Figure 3a and 3b, showing that this particle contains U, Th, Y, and O. The matrix surrounding the particle contains various elements such as Si, Na, Ca, K, O, Al, and Fe. It could not be shown clearly, whether the sample contains lanthanides as well as P. The TOF-SIMS images:  $80 \times 80 \mu\text{m}$ ,  $512 \times 512$  pixel, 275 scans, 6994 s,  $\text{Bi}^{3+}$  are shown in Figure 3a and 3b.

Fig.3a

Fig.3a Sum of: Y +, YO + MC: 40; TC:  $1.733\text{e}^{+005}$  (A)

Sum of: Th +, ThO +, ThO<sub>2</sub>+ MC: 857; TC:  $4.901\text{e}^{+006}$  (B)

Sum of: U +, UO +, UO<sub>2</sub>+ MC: 614; TC:  $2.639\text{e}^{+006}$  (C)

Fig.3b

Fig.3b Overlay of  $\text{UO}_2^+$  (red),  $\text{K}^+$  (blue) and  $^{206}\text{Pb}^+$ ,  $^{207}\text{Pb}^+$ ,  $\text{Pb}^+$  (green)

The  $^{235}\text{U}/^{238}\text{U}$  isotopic ratio of this particle was determined by a SIMS measurement with a high mass resolution. The peak areas  $n_b$  of  $^{235}\text{U}$  and  $^{238}\text{U}$  were determined, as well as the corresponding background areas  $n_0$ , resulting in the net peak area  $s n_n = n_b - n_0$ . The uncertainties are given by  $u(n_b) = \sqrt{n_b}$ ,  $u(n_0) = \sqrt{n_0}$  and  $u(n_n) = \sqrt{n_b + n_0}$  [17]. The data are given in table 2. This results in the isotopic ratio

$$\frac{n_{n,235}}{n_{n,238}} = 0.00755$$

with an uncertainty of

$$u\left(\frac{n_{n,235}}{n_{n,238}}\right) = \frac{n_{n,235}}{n_{n,238}} \sqrt{\frac{u^2(n_{n,235})}{n_{n,235}^2} + \frac{u^2(n_{n,238})}{n_{n,238}^2}} = 0.00014$$

Table 2: Peak areas of  $^{235}\text{U}$  and  $^{238}\text{U}$  are determined by SIMS-measurement ( $20 \times 20 \mu\text{m}$ ,  $32 \times 32$  pixel, 2547 scans, 300 s,  $\text{Bi}^{3+}$ )

Table 2

### $\mu$ -XRF

Due to line overlapping (e.g. RhL, PdL, AgL) and background contents from sample carriers (86.39 wt% Al, 11.03 wt% Pd, 0.21 wt% Mn, 0.2 wt% Fe, 2.17 wt% Cu) and adhesive pads (80.28 wt% Cu, 8.6 wt% Pd, 4.82 wt% Al, 2.17 wt% Mn, 2.32 wt% Fe, 1.08 wt% Si, 0.54 wt% Ca), an exact quantification by  $\mu$ -XRF was not possible. Therefore, results in supplementary information table 3 only show a qualitative comparison of the samples. Especially

uranium could not be detected in the spot measurements.

Fig.4a

The elemental mappings enabled the visualization of particle distributions e.g. for K, Ca, Fe, and Ti. However, the localization of uraniferous particles was not possible with the mentioned parameters. Using long measurement periods per spot, only uranium, thorium, and radium background signals with an average maximum intensity of 10 cps were obtained. Uraniferous particles can possibly be located using optimized measurement periods (long enough to obtain a uranium signal and short enough to eliminate a uranium background signal) and smaller spot distances.

Fig.4b

Figure 4a and 4b: the BSE based SEM image and EDX graph of the measured soil sample.

The minimum required uranium concentrations and particle sizes for a localization and quantification by  $\mu$ -XRF for this type of soil and rock samples should be investigated in further studies.

### Powder XRD

The rock samples collected from Kabul, Afghanistan, are mainly composed of aluminum silicate minerals, such as albite, mica and microcline, with minor phases of other silicate and/or phosphate minerals.

The thorium detected in some samples is primarily in the form of mixed phosphate silicate minerals containing Ca, RE, and Th (possibly also U), such as cheralite. This also means that the thorium in the collected rocks is likely to originate from natural deposits, not from artificial sources, such as weapons. All the acquired diffractograms are given in Fig.1, Fig.2 and Fig.3 of the supplementary information document.

### SEM-EDX

The soil sample measured with SEM in BSE mode revealed a number of heavy particles existing in the sample. Further analyzing these particles by EDX shows that there exist uranium and thorium in significant amounts. The thorium peak is higher than the one of uranium, which can be considered as a further verification for our results indicating higher thorium concentration. Fig.4a and Fig.4b show the BSE based SEM image and EDX graph of the measured soil sample.

## Water samples

The values measured in the first phase differ from one location to the other. Table 3 and Table 4 show the concentration of different elements determined by the ICP-MS and ICP-OES systems, respectively. Samples used in this study are all drinking as well as all-purpose waters, therefore during the evaluation and calculation, international standards for drinking waters are considered. Elements which could not be measured by ICP-MS due to interferences were measured by ICP-OES.

Table 3 ICP-MS results of the first phase samples

Table 3

Table 4 ICP-OES results of the first phase samples

Table 4

The ICP-MS results for the second and third phase samples are shown in Tables 5 and 6 respectively. Where the acronym LDL stands for *Lower than Detection Limit*.

Table 5 ICP-MS results of the second phase samples

Table 5

Table 6 ICP-MS results of the second phase samples

Table 6

In the first measurement phase of, all samples show a lower concentration of uranium than the provisional guideline value (0.03ppm) proposed by WHO [33] except for sample number 8, which was taken from an unconfined well and exhibited a concentration in the range of 0.075 ppm. In some of the samples, aluminum and magnesium concentrations are also higher than

proposed by AUWSSC (see Table 3 in the supplementary information document), but they still are in the range of uncertainty and the permissible limit in the absence of alternate water. For the AUWSSC, the main elements of concern in drinking water are aluminum, zinc, arsenic, and lead.

*Aluminum* is supposed to be an essential element of human nutrition [34]. The value envisaged by WHO and AUWSSC as a concentration standard for aluminum in drinking water is 0.2 ppm [35]. Aluminum concentrations of the water samples analyzed varies from 0.03 to 0.23 ppm, where the maximum value of 0.23 corresponds to sample number 8 number taken from an unconfined well in a village south east of Kabul.

*Zinc* is considered having a harmful effect on living organisms. Elevated intake of Zinc can cause copper deficiency in different age groups, which can be considered as malnutrition [36]. The amount of zinc may differ from surface to sea and tap water. Due to substandard sanitary conditions, the level of zinc is higher in tap and sewer water. The threshold concentration of zinc in drinking water mentioned by WHO for giving water a bad taste and standard value proposed by AUWSSC is 3 ppm [37]. In the samples measured in this study the concentration of zinc was far below the above mentioned guideline by WHO and AUWSSC, it ranged from 0.0003 to 0.13 ppm.

*Arsenic* can appear in organic and inorganic form in water, with inorganic arsenic compounds being the most probable form in drinking water having a relatively high level of toxicity [38]. The provisional guideline value for arsenic in drinking water given by WHO and adopted by AUWSSC is 0.01 ppm [39], while the concentration in this study varied from 0.001 to 0.003ppm, which is clearly below the limit.

*Lead* as a poisonous and most abundant heavy metal is considered highly toxic for human beings [40]. The provisional guideline value of lead in drinking water recommended by WHO and adopted by AUWSSC is 0.01 ppm [41]. Lead concentrations in our samples were far below this value, ranging from 0.006 to 0.0012 ppm.

*Uranium* is not a necessary nutrient for humans and animals [42], but when ingested it appears rapidly in the blood stream and associates itself with red blood

cells [43]. The provisional guideline value for uranium in drinking water proposed by WHO and adopted by AUWSSC is 0.03 ppm or 30 ppb [33]. Uranium concentrations of our samples ranged between 0.01 to 26.07 ppb which corresponds to the sample number 12 and sample number 1 of the second and third phase, respectively. All of the samples measured in this study exhibited uranium concentrations below the recommended limit.

*Thorium*: There is less information available on thorium health effects on human in comparison to uranium, but studies on animals show that ingestion of massive amounts of thorium causes metal poisoning leading to death [44]. The proposed guidance level of thorium in drinking water is 0.1 ppb [45], while thorium concentration in our samples ranged between 2 and 154 ppb.

*Radium* as a decay product of uranium and thorium is also not necessary for living organisms and causes adverse health effects upon incorporation. Under acidic conditions radium easily dissolves in groundwater. Extensive doses of radium cause bone cancer [46]. In our samples, no detectable amounts of radium were measured.

In the water samples we analyzed, uranium and thorium were found in considerable amounts, as can be seen in Table 5. Uranium concentrations of all samples are still below the 30 ppb guideline value proposed by WHO [33]. Thorium concentration can be as high as 100 ppm in waters enriched with humic substances [45]. In the second phase of our study, the concentrations of one sample was as high as 154 ppm (sample number 1), with rather large uncertainty. The water source at this location is near a sewage water reservoir and vines and leakages from the reservoir to the well are likely. This might have caused a change in pH of the water causing thorium to hydrolyze leading in turn to a higher apparent solubility and increased concentration of thorium in the water [47]. Lead concentrations of all samples were well below the WHO guideline values and, except for number 6, also below the detection limit.

Results of the water sampled in the third phase revealed concentrations of thorium and lead below detection limit (LDL; see Table 6). Only for uranium,

considerable amounts were detected in the samples. However, also uranium concentrations are below the WHO guideline value of 30 ppb.

## Conclusions

Looking at chronological and geological information about the sampling area, all different techniques used for the measurements and analyses indicate that the soil and rock samples have an enhanced radioactivity level as compared to global mean values and also compared to that of normal rocks found elsewhere in Afghanistan. Gamma and alpha spectroscopy results show that the thorium concentration is higher than that of uranium, which is verified by PXRD measurements. PXRD also reveals that the presence of considerable amounts of thorium is due to the mineralogical structure of the samples containing cheralite.

The detection of uranium in our samples, which could not be determined by gamma spectroscopy, indicates that due to higher interference and attenuation probability, gamma spectroscopy is not the optimal technique for quantifying the uranium concentration in this case. Instead, alpha spectroscopy and SIMS yielded plausible values. For the risk assessment, nevertheless, also uranium of natural isotope ratio needs to be considered. Keeping in mind the special geological and mineralogical structure, higher radon concentration in caves and basements and the enhanced radioactivity in the area were reported [23, 48] and require restrictions on use for human housing in some locations.

The element concentrations of water samples collected in the first phase of the study all remained below the recommended guideline values, except for sample number 8. Thus, it can be concluded that the drinking water supplied by AUWSSC in Kabul is in good condition concerning its level of hazardous toxic elements. Water sample number 8 was collected in a village with agriculture and livestock farming, including use of farmyard manure and chemical fertilizers. Enhanced uranium concentration in the well water may be related to the presence of nitrate deriving from fertilizers, which causes oxidation of uranium, and thus mobilization and leaching to the ground water [49], meanwhile uranium from phosphate fertilizers is reported to disturb the ratio of its daughter nuclides [50]. Samples collected in the second phase showed a low concentration of uranium and lead, whereas

measurement of thorium resulted in relatively high concentrations in samples number 1 and 20. However, due to the large uncertainty of the measurements, it is impossible to decide, whether the concentration is really higher than would be expected. In the third phase, all element concentrations remained below the recommended guideline values, thus the water quality meets the requirements concerning U, Th, Ra and Pb concentrations. Meanwhile the highest uranium concentration recorded by Banks et al. (2014) in Faryab province of northern Afghanistan was 62 ppb from dug wells in Qurgan and Andkhoi. Groundwater uranium concentrations were found to increase towards the north of the province, which may indicate that uranium anionic complexes are susceptible to the same evapoconcentrative processes as many other soluble elements. Alternatively, the high concentrations of uranium in saline ground waters may be mobilized by complexation with salinity-related species, such as sulphate. A much stronger correlation was found with sulphate compared to chloride. Uranium minerals within igneous or metamorphic rocks (e.g. apatite, zircon), uranium within dark organic sedimentary marine mud rocks and shales and inorganic fertilizers, especially those derived from apatite, are suggested as ultimate sources of uranium [51].

The widespread distribution of  $^{238}\text{U}$  and thus, the widespread distribution of its daughter products such as  $^{226}\text{Ra}$ , as compared to thorium, is caused by its relatively high solubility. Thus, the progeny of  $^{238}\text{U}$ ,  $^{226}\text{Ra}$ , is commonly found in ground water. The geochemical properties of  $^{226}\text{Ra}$  differ from those of  $^{238}\text{U}$ , however, co-occurrence is not common [52] because the degree and chemical conditions of mobilization of the parent  $^{238}\text{U}$  and product  $^{226}\text{Ra}$  are different [53]. It might also be possible that radium is absorbed during migration to the sampling site.

Considering 3 liters of drinking water consumption for an adult per day, the average annual effective dose for uranium, thorium and radium was estimated in sample 8 of the first phase and sample 1 and 20 of the second phase with highest concentrations as 0.07mSv/a, 0.19 mSv/a and 0.03 mSv/a respectively, which is still under the recommended dose level by IAEA for the member of public.

## Acknowledgments

The authors would like to thank their colleagues from AAEHC and AUWSSC) for collaboration in collecting samples; Mohammad Tanha is grateful to the Siebold Sasse foundation for the financial support of his PhD.

## References

1. UNSCEAR. *Sources and effects of ionizing radiation: United Nations Scientific Committee on the Effects of Atomic Radiation UNSCEAR 2000 report to the General Assembly, with scientific annexes*. New York: United Nations; 2000.
2. Dinh Chau N, Dulinski M, Jodlowski P, et al. Natural radioactivity in groundwater – a review. *Isotopes in Environmental and Health Studies*. 2011;47(4):415-437. doi:10.1080/10256016.2011.628123.
3. Ghosh D, Deb A, Bera S, et al. Measurement of natural radioactivity in chemical fertilizer and agricultural soil: evidence of high alpha activity. *Environmental Geochemistry and Health*. 2008;30(1):79-86. doi:10.1007/s10653-007-9114-0.
4. IAEA TECDOC. *Radioactive Particles in the Environment: Sources, Particle Characterization and Analytical Techniques*. 2011. [http://www-pub.iaea.org/MTCD/Publications/PDF/TE\\_1663\\_web.pdf](http://www-pub.iaea.org/MTCD/Publications/PDF/TE_1663_web.pdf).
5. Mohmand et al. *Reports on geophysical studies of Kabul suburbs (report in Dari)*. Kabul; 1987.
6. AGS and AAEHC. *Radiometric studies and illegal housing in Kabul and suburbs: Afghanistan Geological Survey and Afghan Atomic Energy High Commission collaboration reports*. [Internal collaboration report for internal use only]. Kabul; 2010-2012.
7. Durakovic A. Undiagnosed illnesses and radioactive warfare. *Croatian medical journal*. 2003;44(5):520-532.
8. Burton et al. *Stormwater effects handbook: A toolbox for watershed managers, scientists and engineers / G. Allen Burton, Jr. and Robert E. Pitt*. Boca Raton, Fla.: Lewis Publishers; 2002.
9. World Bank. *Afghanistan - Kabul Municipal Development Program: Implementation Status Results Report : Sequence 03*; 2015. The World Bank; ISR18804. <http://www-wds.worldbank.org/external/default/WDSContentServer/WDS/...>
10. Fawell J. Contaminants in drinking water. *British Medical Bulletin*. 2003;68(1):199-208. doi:10.1093/bmb/ldg027.
11. Zapecza et al. *Natural Radioactivity in Ground Water: A Review*. Washington, USA: U.S. Geological Survey. 1986.
12. Mohmand et al. *Schematic of Kabul and suburbs gamma anomaly*. Kabul: Afghanistan Geological Survey; 1987.
13. *FitzPeaks*. Oxfordshire, UK: Jim Fitzgerald; 2014.
14. *QtiPlot*. Bucharest, Romania: Gadiou, Roger; Franke, Knut; 2010.
15. Papadopoulos A, Christofides G, Koroneos A, et al. Radioactive secular equilibrium in <sup>238</sup>U and <sup>232</sup>Th series in granitoids from Greece. *Applied Radiation and Isotopes*. 2013;75:95-104. doi:10.1016/j.apradiso.2013.02.006.
16. Lieser KH. *Nuclear and Radiochemistry: Fundamentals and Applications*. Weinheim: Wiley-VCH; 2001.
17. BIPM. *Evaluation of measurement data — Guide to the expression of uncertainty in measurement of uncertainty in measurement*. JCGM 100. Paris, France: BIPM. 2008. Updated 2008.
18. Eichrom Technologies. Inc. *Uranium and Thorium in Water. Analytical Procedures*. Lisle, USA. 2013. Updated 2013.
19. Bister S, Koenn F, Bunka M, et al. Uranium in water of the Mulde River. *J Radioanal Nucl*



- Chem. 2010;286(2):367-372.  
doi:10.1007/s10967-010-0767-2.
20. Eichrom Technologies. Inc. *Uranium and Thorium in Water. Analytical Procedures*. Lisle, USA. 2001. Updated 2001.
  21. Eckert & Ziegler Nuclitec GmbH. *RADIOACTIVE SOLUTIONS AND GASES*. Berlin, Germany: Eckert & Ziegler Nuclitec GmbH.
  22. Inorganic Ventures. Inorganic standards and custom reference materials.  
<https://www.inorganicventures.com/periodic-table>.
  23. Wolfart W. *Geologie Von Afghanistan*: Gebrüder Borntraeger  
Verlagsbuchhandlung, Science Publishers; 1980.  
<https://books.google.de/books?id=cNRMvgAACAAJ>.
  24. Andritzky G. Das Kristallin im Gebiet Panjao-Kabul-Jalalabad (Zentral- und Ost-Afghanistan). 1971;96(Geologisches).
  25. IAEA. *Uranium deposits in magmatic and metamorphic rocks: Proceedings of a Technical Committee Meeting on Uranium Deposits in Magmatic and Metamorphic Rocks / organized by the International Atomic Energy Agency ... held in Salamanca, ... 1986*. Vienna: International Atomic Energy Agency; 1989. Panel proceedings series.
  26. Faryad SW, Collett S, Finger F, et al. The Kabul Block (Afghanistan), a segment of the Columbia Supercontinent, with a Neoproterozoic metamorphic overprint. *Gondwana Research*. 2016;34:221-240.  
doi:10.1016/j.gr.2015.02.019.
  27. Eisenbud M, Gesell TF. *Environmental radioactivity: From natural, industrial, and military sources*. 4th ed. San Diego, Calif., London: Academic Press; 1997.
  28. Bundesamt für Strahlenschutz. *Umweltradioaktivität und Strahlenbelastung: Jahresbericht*. München; 2014.
  29. Sohrabi M, Durrani S, Ahmed J, eds. *HIGH LEVELS OF NATURAL RADIATION: Proceedings of an International Conference Ramsar, 3-7 November 1990*. Vienna: IAEA; 1990.
  30. Minter M, Winkler P, Wyatt B, et al. Reliability of using <sup>238</sup>U/<sup>235</sup>U and <sup>234</sup>U/<sup>238</sup>U ratios from alpha spectrometry as qualitative indicators of enriched uranium contamination. *Health physics*. 2007;92(5):488-495.  
doi:10.1097/01.HP.0000254847.21026.7c.
  31. Bottrell SH. Redistribution of uranium by physical processes during weathering and implications for radon production. *Environmental Geochemistry and Health*. 1993;15(1):21-25. doi:10.1007/BF00146289.
  32. Siddeeg SEMB, Livens F. *Geochemistry of natural radionuclides in uranium-enriched river catchments*. Great Britain: University of Manchester; 2013.  
<http://www.manchester.ac.uk/escholar/uk-ac-man-scw:198785>.
  33. WHO. *Uranium in Drinking-water: Background document for development of WHO Guidelines for Drinking-water Quality*. Geneva; 2011.
  34. Hathcock J. *Nutritional Toxicology*: Elsevier Science; 2012; v. 1.  
<https://books.google.de/books?id=cyl0aUDLgoC>.
  35. WHO. *Aluminium in drinking-water: Background document for development of WHO Guidelines for Drinking-water Quality*. Geneva; 2010.
  36. Plum LM, Rink L, Haase H. The essential toxin: impact of zinc on human health. *International journal of environmental research and public health*. 2010;7(4):1342-1365. doi:10.3390/ijerph7041342.
  37. WHO. *Zinc in Drinking-water: Background document for development of WHO*

- Guidelines for Drinking-water Quality*. Geneva; 2003.
38. WHO. *PREVENTING DISEASE THROUGH HEALTHY ENVIRONMENTS: EXPOSURE TO ARSENIC: A MAJOR PUBLIC HEALTH CONCERN*. Geneva; 2010.
  39. WHO. *Arsenic in Drinking-water: Background document for development of WHO Guidelines for Drinking-water Quality*. Geneva; 2011.
  40. Hunter P. A toxic brew we cannot live without. Micronutrients give insights into the interplay between geochemistry and evolutionary biology. *EMBO Rep*. 2008;9(1):15-18. doi:10.1038/sj.embor.7401148.
  41. WHO. *Lead in Drinking-water: Background document for development of WHO Guidelines for Drinking-water Quality*. Geneva; 2011.
  42. Virginia C, Resources CE, Resources B, et al. *Uranium Mining in Virginia: Scientific, Technical, Environmental, Human Health and Safety, and Regulatory Aspects of Uranium Mining and Processing in Virginia*: National Academies Press; 2012. <https://books.google.de/books?id=5oh2AKZn3c0C>.
  43. Karpas. *Analytical Chemistry of Uranium*; 2014.
  44. Prasad M. *Trace Elements as Contaminants and Nutrients: Consequences in Ecosystems and Human Health*: Wiley; 2008. <https://books.google.de/books?id=FRJsxgZXxUMC>.
  45. Boyle RW. *Geochemical prospecting for thorium and uranium deposits*. Amsterdam: Elsevier; 1982. Developments in economic geology; 16. <http://www.elsevier.com/journal>.
  46. Finkelstein et al. Radium in drinking water and risk of bone cancer in Ontario youths: A second study and combined analysis. *Occupational and environmental medicine*. 1996;53(5):305-311.
  47. Kobets SA, Pshinko GN. Factors affecting forms of finding Th(IV) in aqueous solutions. *J. Water Chem. Technol*. 2014;36(2):51-55. doi:10.3103/S1063455X14020015.
  48. Tanha M, Vahlbruch J-W, Riebe B, et al. Activity concentration and annual assessment of Radon dose in Afghanistan using an active radon exposure meter. 2017.
  49. Nolan et al. Natural Uranium Contamination in Major U.S. Aquifers Linked to Nitrate. *Environ. Sci. Technol. Lett*. 2015;2(8):215-220. doi:10.1021/acs.estlett.5b00174.
  50. Komura K, YANAGISAWA M, SAKURAI J, et al. Uranium, thorium and potassium contents and radioactive equilibrium states of the uranium and thorium series nuclides in phosphate rocks and phosphate fertilizers. *RADIOISOTOPES*. 1985;34(10):529-536. doi:10.3769/radioisotopes.34.10\_529.
  51. Banks et al. *Hydrogeological Atlas of Faryab Province: Northern afghanistan*. Kabul: Ministry of Rural Rehabilitation & Development; 2014.
  52. Szabó et al. Geologic and geochemical factors controlling uranium, radium-226, and radon-222 in ground water: Newark Basin, New Jersey, in Coalfields of New Mexico. [Geology and Resource]. 1992.
  53. Focazio MJ, Szabo Z, Kraemer TF, Mullin AH. *Occurrence of Selected Radionuclides in Ground Water Used for Drinking Water in the United States: A Targeted Reconnaissance Survey, 1998*. Washington, USA; 2001. <https://pubs.usgs.gov/wri/wri004273/pdf/wri004273.pdf>.

Phase	Activity [Bq/kg]	<sup>238</sup> U	<sup>226</sup> Ra	<sup>227</sup> Ac	<sup>228</sup> Ra	<sup>228</sup> Th	<sup>40</sup> K
1st	Max	28660 ± 1670	10700 ± 400	540 ± 100	203000 ± 8000	212000 ± 6200	15230 ± 845
	Min	1200 ± 112	1300 ± 175	68 ± 7	1900 ± 100	195 ± 10	273 ± 50
2nd	Max	33500 ± 6600	38300 ± 7100	3900 ± 600	347000 ± 28000	383000 ± 30500	24700 ± 1300
	Min	167 ± 57	55 ± 5	84 ± 8	90 ± 10	75 ± 10	615 ± 68
3rd	Max	LDL	270 ± 11	LDL	6000 ± 680	5900 ± 670	4950 ± 300
	Min	LDL	20 ± 1	LDL	177 ± 17	147 ± 14	400 ± 40

Table 1

	$n_b$	$u(n_b)$	$n_0$	$u(n_0)$	$n_n$	$u(n_n)$
$^{235}\text{U}$	2817	53,075	16	4,000	2801	53,23
$^{238}\text{U}$	371011	609,107	178	13,342	370833	609,25

Table 3

Sample Standard	Element concentration measured by ICP-MS [ppm]							
	Zinc	Arsenic	Nickel	Manganese	Copper	Chromium	Barium	Aluminum
1	0.14	0.003	0.002	0.001	0.002	0.005	0.05	0.032
2	0.03	0.004	0.002	0.007	0.003	0.005	0.05	0.11
3	0.08	0.004	0.002	0.006	0.003	0.005	0.05	0.13
4	0.001	0.005	0.002	0.002	0.002	0.004	0.03	0.10
5	0.0005	0.002	0.01	0.001	0.002	0.003	0.03	0.11
6	0.003	0.002	0.01	0.001	0.002	0.003	0.03	0.13
7	0.001	0.002	0.01	0.001	0.004	0.003	0.02	0.1
8	0.0003	0.001	0.002	0.0008	0.003	0.002	0.08	0.23

Table 3

Sample	Element concentration measured by ICP-OES [ppm]						
	Na	Ca	Fe	K	Pb	Mg	U
1	36±1	55±0.4	0.00015±0.0001	8±0.2	0.0012±0.0002	22±0.1	0.0204±0.0117
2	55.±1	63±0.3	0.0002±0.0001	11±0.4	0.0009±0.0004	36±0.1	0.0229±0.0048
3	42±1	57±0.4	0.00055±0.0001	8±0.2	0.0011±0.0004	26±0.1	0.0177±0.0209
4	10±0.2	41±0.4	LDL	6±0.2	0.0001±0.0002	12±0.1	0.0240±0.0277
5	99±0.4	15±0.1	0.0001±0	11±0.2	0.0005±0.0006	103±0.00	0.0094±0.023
6	97±0.0	17±0.2	0.00015±0.0001	12±0.2	0.0001±0.0003	100±1	0.0091±0.0039
7	96±0.3	13 ±0.12	0.00015±0	12±0.2	0.0002±0.0001	101±0.3	0.0100±0.013
8	64±0.5	55±0.03	0.00065±0.0002	20±0.5	0.0006±0.0003	51±0.3	0.0748±0.0186

Table 4

Sample	U [ppb]	Th [ppb]	Pb [ppb]
1	9±14	154 ±7	LDL
2	21±17	38 ±5	LDL
3	5 ±4	70 ±44	LDL
4	4±5	10 ±12	LDL
5	0.06±0.04	2 ±0	LDL
6	9±7	28 ±11	2±5
7	5±1	10 ±3	LDL
8	4±4	4 ±1	LDL
9	4±3	2 ±0	LDL
10	4±2	2 ±0	LDL
11	5±4	4 ±1	LDL
12	0.01±0.01	LDL	LDL
13	6±4	24 ±19	LDL
14	2±2	2 ±0	LDL
15	5±4	10 ±3	LDL
16	7±5	4 ±1	LDL
17	4±3	14 ±14	LDL
18	4±2	8 ±8	LDL
19	6±3	LDL	LDL
20	0.04±0.14	2 ± 0	LDL
21	1±2	12 ±15	LDL
22	0.18±0.05	4 ±6	LDL

23	10±3	4 ±1	LDL
----	------	------	-----

Table 5



Sample	U [ppb]	Th [ppb]	Pb [ppb]
1	26 ±10	LDL	LDL
2	4±3	LDL	LDL
3	4±2	LDL	LDL
4	16±4	LDL	LDL
5	20±20	LDL	LDL
6	3±10	LDL	LDL
7	3±2	LDL	LDL
8	3±3.11	LDL	LDL
9	11±10	LDL	LDL
10	2±2	LDL	LDL
11	0.3±0.6	LDL	LDL
12	1±4	LDL	LDL
13	1±1	LDL	LDL
14	6±4	LDL	LDL
15	1±1	LDL	LDL
16	2±3	LDL	LDL
17	2±1	LDL	LDL
18	7±5	LDL	LDL
19	3±3	LDL	LDL
20	7±6	LDL	LDL

Table 6

## Supplementary information

**Table 1** detailed information on the source type, location and situation of samples

Phase	Sample type and Number	Background [c/sec]	Location's local name	GPS coordinates	Mass [g]	Measurement date
1 <sup>st</sup> Phase – January 2014	Rock 1	~ 50	Alikhail Hills Deh sabz distrect, Kabul	N 34.57243 <sup>0</sup> E 69.26254 <sup>0</sup>	110.5	7/2/2014
	Rock 2	~ 50	Khawja Rawash Khair Khana, Kabul	N 34.59268 <sup>0</sup> E 69.20026 <sup>0</sup>	118	7/24/2014
	Rock 3	~ 50	Khawja Rawash Khair Khana, Kabul	N 34.59306 <sup>0</sup> E 69.19986 <sup>0</sup>	147.6	7/28/2014
	Rock 4	~ 50	Khawja Rawash Khair Khana, Kabul	N 34.57244 <sup>0</sup> E 69.26255 <sup>0</sup>	172.5	7/14/2014
	Soil 5	~ 50	Alikhail Hills Deh sabz distrect, Kabul	N 34.57242 <sup>0</sup> E 69.26253 <sup>0</sup>	43.2	7/14/2014
2 <sup>nd</sup> Phase – October 2014	Rock 1	~ 50	Daf-e-hawa hills, Kabul	N 34.34161 <sup>0</sup> E 69.16236 <sup>0</sup>	103.84	6/4/2015
	Rock 2	~ 45	Daf-e-hawa hills, Kabul	N 34.34164 <sup>0</sup> E 69.16252 <sup>0</sup>	91.29	3/26/2015

Rock 3	~ 45	Daf-e-hawa hills, Kabul	N 34.34208 <sup>0</sup> E 69.15451 <sup>0</sup>	94.06	6/5/2015
Rock 4	~ 40	Qasaba hills, Kabul	N 34.35335 <sup>0</sup> E 69.1214 <sup>0</sup>	152.08	3/27/2015
Rock 5	~ 40	Qasaba hills, Kabul	N 34.35337 <sup>0</sup> E 69.1212 <sup>0</sup>	101.05	6/5/2015
Rock 6	~ 40	Qasaba hills, Kabul	N 34.35349 <sup>0</sup> E 69.11594 <sup>0</sup>	93.66	6/5/2015
Rock 7	~ 40	Alli khail hills, Kabul	N 34.3685 <sup>0</sup> E 69.11374 <sup>0</sup>	85.98	6/8/2015
Rock 8	~ 40	Qasaba hills, Kabul	N 34.35351 <sup>0</sup> E 69.11596 <sup>0</sup>	141.46	3/30/2015
Rock 9	~ 40	Qasaba hills, Kabul	N 34.35353 <sup>0</sup> E 69.11598 <sup>0</sup>	165.17	3/31/2015
Rock 10	~ 40	Qasaba hills 315 Army base, Kabul	N 34.35335 <sup>0</sup> E 69.12016 <sup>0</sup>	117.96	8/6/2015
Rock 11	~ 40	Qasaba hills 315 Army base, Kabul	N 34.35351 <sup>0</sup> E 69.11594 <sup>0</sup>	94.08	4/7/2015
Rock 12	~ 40	Qasaba hills 315 Army base, Kabul	N 34.35349 <sup>0</sup> E 69.11595 <sup>0</sup>	91.67	9/6/2015
Rock 13	~ 40	Qasaba hills 315 Army base, Kabul	N 34.35357 <sup>0</sup> E 69.11597 <sup>0</sup>	100.73	4/8/2015
Rock 14	~ 40	Ali Khail deh sabz, Kabul	N 34.34207 <sup>0</sup> E 69.15451 <sup>0</sup>	99.32	3/28/2015
Rock 15	~ 40	Ali Khail deh sabz, Kabul	N 34.33093 <sup>0</sup>	102.07	6/6/2015

				E 69.02350 <sup>0</sup>		
	Rock 16	~ 40	Qasaba hills 315 Army base, Kabul	N 34.35352 <sup>0</sup> E 69.11594 <sup>0</sup>	95.78	4/9/2015
	Rock 17	~ 40	Ali Khail deh sabz, Kabul	N 34.34205 <sup>0</sup> E 69.15449 <sup>0</sup>	94.38	10/6/2015
	Rock 18	~ 40	Qasaba hills, Kabul	N 34.35352 <sup>0</sup> E 69.11596 <sup>0</sup>	151.3	4/10/2015
	Rock 19	~ 40	Qasaba hills, Kabul	N 34.35350 <sup>0</sup> E 69.11591 <sup>0</sup>	95.03	10/6/2015
	Rock 20	~ 40	Qasaba hills, Kabul	N 34.35349 <sup>0</sup> E 69.11591 <sup>0</sup>	150.88	4/13/2015
3 <sup>rd</sup> Phase – October 2015	Rock 1	~ 45	Koh-e-Asmai (Front lower right), Kabul	N 34.525105 E 69.151523	108.44	3/7/2016
	Rock 2	~ 45	Koh-e-Asmai (Front Lower right), Kabul	N 34.525083 <sup>0</sup> E 69.151602 <sup>0</sup>	105.69	3/8/2016
	Rock 3	~ 50	Koh-e-Asmai (Front lower right), Kabul	N 34.525131 <sup>0</sup> E 69.151777 <sup>0</sup>	103.44	3/14/2016
	Rock 4	~ 40	Koh-e-Asmai (Front lower middle), Kabul	N 34.525212 <sup>0</sup> E 69.152060 <sup>0</sup>	114.93	3/15/2016

	Rock 5	~ 40	Koh-e-Asmai (Front lower middle), Kabul	N 34.525231 <sup>0</sup> E 69.152231 <sup>0</sup>	106.42	3/16/2016
	Rock 6	~ 40	Koh-e-Asmai (Front lower middle), Kabul	N 34.525269 <sup>0</sup> E 69.152425 <sup>0</sup>	105.42	3/17/2016
	Rock 7	~ 40	Koh-e-Asmai (Front lower left), Kabul	N 34.525331 <sup>0</sup> E 69.152885 <sup>0</sup>	107.73	3/18/2016
	Rock 8	~ 40	Koh-e-Asmai (Front lower left), Kabul	N 34.525336 <sup>0</sup> E 69.153052 <sup>0</sup>	107.33	3/21/2016
	Rock 9	~ 40	Koh-e-Asmai (Front lower left), Kabul	N 34.525317 <sup>0</sup> E 69.153156 <sup>0</sup>	104.1	3/21/2016
	Rock 10	~ 40	Koh-e-Asmai (Front lower edge), Kabul	N 34.525085 <sup>0</sup> E 69.153425 <sup>0</sup>	114.41	3/22/2016
	Rock 11	~ 40	Koh-e-Asmai (Front upper edge), Kabul	N 34.525076 <sup>0</sup> E 69.153328 <sup>0</sup>	109.22	3/23/2016

	Rock 12	~ 40	Koh-e-Asmai(Front upper left), Kabul	N 34.525093 <sup>0</sup> E 69.152969 <sup>0</sup>	104.46	3/23/2016
	Rock 13	~ 40	Koh-e-Asmai(Front upper middle), Kabul	N 34.524957 <sup>0</sup> E 69.152449 <sup>0</sup>	114.47	3/24/2016
	Rock 14	~ 40	Koh-e-Asmai (Front upper right), Kabul	N 34.524778 <sup>0</sup> E 69.152135 <sup>0</sup>	107.1	3/24/2016
	Rock 15	~ 40	Koh-e-Asmai (Back upper right), Kabul	N 34.524697 <sup>0</sup> E 69.152006 <sup>0</sup>	107.64	3/29/2016
	Rock 16	~ 40	Koh-e-Asmai (Back upper middle), Kabul	N 34.524464 <sup>0</sup> E 69.151723 <sup>0</sup>	106.43	3/29/2016
	Rock 17	~ 40	Koh-e-Asmai (Back upper left), Kabul	N 34.524164 <sup>0</sup> E 69.151453 <sup>0</sup>	111.02	3/30/2016
	Rock 18	~ 40	Koh-e-Asmai (Back lower right), Kabul	N 34.523960 <sup>0</sup> E 69.150879 <sup>0</sup>	111.85	3/30/2016

	Rock 19	~ 40	Koh-e-Asmai (Back lower middle), Kabul	N 34.523951 <sup>0</sup> E 69.149862 <sup>0</sup>	112.91	3/31/2016
	Rock 20	~ 40	Koh-e-Asmai (Back lower left), Kabul	N 34.523648 <sup>0</sup> E 69.147780 <sup>0</sup>	105.01	3/31/2016
	Rock 21	~ 40	Koh-e-Sher Darwazah (Front lower right), Kabul	N 34.509712 <sup>0</sup> E 69.164546 <sup>0</sup>	106	4/1/2016
	Rock 22	~ 40	Koh-e-Sher Darwazah (Front lower middle), Kabul	N 34.509361 <sup>0</sup> E 69.164596 <sup>0</sup>	106.69	4/4/2016
	Rock 23	~ 40	Koh-e-Sher Darwazah (Front lower left), Kabul	N 34.509569 <sup>0</sup> E 69.163939 <sup>0</sup>	104.29	4/4/2016
	Rock 24	~ 40	Koh-e-Sher Darwazah (Front upper left), Kabul	N 34.509009 <sup>0</sup> E 69.163946 <sup>0</sup>	110.67	4/5/2016
	Rock 25	~ 40	Koh-e-Sher Darwazah (Front upper left), Kabul	N 34.509177 <sup>0</sup> E 69.163680 <sup>0</sup>	105.36	4/5/2016

	Rock 26	~ 40	Koh-e-Sher Darwazah (Front lower left), Kabul	N 34.508967 <sup>0</sup>  E 69.163729 <sup>0</sup>	107.85	4/6/2016
--	---------	------	--	--	--------	----------

**Table 1**

**Table 2** detailed information on the source type, location and situation of samples

Phase	Sample #	Location's local name	GPS coordinates	Source	Source condition
1 <sup>st</sup> Phase – January 2014	1-2	Supply Zone #5 Sara Mina, Kabul	N 34.583587 <sup>0</sup> E 69.146035 <sup>0</sup>	Main well	The well is fully covered and the sample was taken directly from the sterilized open end of pipe (Water Tap) and stored in sterilized plastic bottle.
	1-3	Supply Zone #5, 500 Families, Kabul	N 34.584319 <sup>0</sup> E 69.149953 <sup>0</sup>	Well #4	The well is fully covered and the sample was taken directly from none sterilized open end of pipe (Water Tap) and stored in sterilized plastic bottle.
	1-4	Supply Zone #5 Prozha -e- Jadeed, Kabul	N 34.599752 <sup>0</sup> E 69.136561 <sup>0</sup>	Well #500	The well is fully covered and the sample was taken directly from none sterilized open end of pipe (Water Tap) and stored in sterilized plastic bottle.
	1-5	Supply Zone #5, Sarai -e-	N 34.584485 <sup>0</sup> E 69.129325 <sup>0</sup>	Well # 3000	The well is partially covered and the sample was taken



	Shamalee, Kabul			directly from none sterilized open end of pump (Water Tap) and stored in sterilized plastic bottle.
1-6	Supply Zone #1, Kart -e- Naw, Kabul	N 34.512691 <sup>0</sup> E 69.232279 <sup>0</sup>	Well # 1000	The well is partially covered and the sample was taken directly from the well and stored in sterilized plastic bottle.
1-7	Supply Zone #1 Bagrami Dist, Kabul	N 34.497945 <sup>0</sup> E 69.261243 <sup>0</sup>	50 m from booster pump station	The sample was taken directly from sterilized open end of a residential area water pipe (Water Tap) and stored in sterilized plastic bottle.
1-8	Supply Zone #1 Bagrami Dist, Kabul	N 34.497213 <sup>0</sup> E 69.260795 <sup>0</sup>	Booster pump station	The well is totally tight covered and the sample was taken directly from sterilized open end (Water Tap) of booster pipe and stored in sterilized plastic bottle.
2-1	Chahar asiaab Dist. Kabul	N 34.382938 <sup>0</sup> E 69.145745 <sup>0</sup>	Residentia l area well	The well is totally open and the sample was taken directly from the well and stored in sterilized plastic bottle.

2 <sup>nd</sup> Phase – October 2014	2-2	Qala Safeed – Char Asyab, Kabul	N 34.379617 <sup>0</sup> E 69.130564 <sup>0</sup>	Hand pump	Even the pump was fully covered but there was still possibility for pollutants to get in
	2-3	Qala Safeed – Char Asyab, Kabul	N 34.379793 <sup>0</sup> E 69.129744 <sup>0</sup>	Hand pump	Even the pump was fully covered but there was still possibility for pollutants to get in
	2-4	Qala Ata Mohammad Khan – Char Asyab, Kabul	N 34.379034 <sup>0</sup> E 69.144666 <sup>0</sup>	Open well	The well was totally open and pollutants can easily get in, buckets were used to get water out of the well
	2-5	Qala Luqman – Char Asyab, Kabul	N 34.368456 <sup>0</sup> E 69.140964 <sup>0</sup>	Open well	The well was totally open and pollutants can easily get in, buckets were used to get water out of the well
	2-6	Alaudeen, Kabul	N 34.495190 <sup>0</sup> E 69.137227 <sup>0</sup>	City water supply	The water comes from fully covered city water supply tanks
	2-7	Lis-e- Habibiah Kabul	N 34.500378 <sup>0</sup> E 69.150765 <sup>0</sup>	Open well	The well was totally open and pollutants can easily get in, buckets were used to get water out of the well
	2-8	Qala-e-Logar, Kabul	N 34.445127 <sup>0</sup> E 69.139006 <sup>0</sup>	Open well	The well was totally open and pollutants can easily get in,

					buckets were used to get water out of the well
2-9	Qala-e-Logar, Kabul	N 34.445810 <sup>0</sup> E 69.139698 <sup>0</sup>	Open well		The well was totally open and pollutants can easily get in, buckets were used to get water out of the well
2-10	Qala-e-Logar, Kabul	N 34.444948 <sup>0</sup> E 69.138926 <sup>0</sup>	Hand pump		Even the pump was fully covered but there was still possibility for pollutants to get in
2-11	Qala-e-Logar, Kabul	N 34.446606 <sup>0</sup> E 69.141067 <sup>0</sup>	Hand pump		Even the pump was fully covered but there was still possibility for pollutants to get in
2-12	Qala-e-Logar, Kabul	N 34.447110 <sup>0</sup> E 69.140199 <sup>0</sup>	Open well		The well was totally open and pollutants can easily get in, buckets were used to get water out of the well
2-13	Qala-e-Logar, Kabul	N 34.447097 <sup>0</sup> E 69.140955 <sup>0</sup>	Hand pump		Even the pump was fully covered but there was still possibility for pollutants to get in
2-14	Haji bakhshi village, Shaker darah Kabul	N 34.685577 <sup>0</sup> E 69.078843 <sup>0</sup>	Open well		The well was totally open and pollutants can easily get in,

					buckets were used to get water out of the well
2-15	Haji bakhshi village, Shaker darah Kabul	N 34.685892 <sup>0</sup> E 69.077787 <sup>0</sup>	Open well		The well was totally open and pollutants can easily get in, buckets were used to get water out of the well
2-16	Haji bakhshi village, Shaker darah Kabul	N 34.684996 <sup>0</sup> E 69.078092 <sup>0</sup>	Open well		The well was totally open and pollutants can easily get in, buckets were used to get water out of the well
2-17	Haji bakhshi village, Shaker darah Kabul	N 34.684776 <sup>0</sup> E 69.080279 <sup>0</sup>	Open well		The well was totally open and pollutants can easily get in, buckets were used to get water out of the well
2-18	Haji bakhshi village, Shaker darah Kabul	N 34.684507 <sup>0</sup> E69.077795 <sup>0</sup>	Open well		The well was totally open and pollutants can easily get in, buckets were used to get water out of the well
2-19	Haji bakhshi village, Shaker darah Kabul	N 34.685950 <sup>0</sup> E 69.076257 <sup>0</sup>	Open well		The well was totally open and pollutants can easily get in, buckets were used to get water out of the well
2-20	Haji bakhshi village, Shaker darah Kabul	N 34.687201 <sup>0</sup> E 69.080225 <sup>0</sup>	Open spring		The spring is not covered by anything, human; animals and

					pets used it as drinking water source
	2-21	KINLEY mineral water by Coca Cola Company	N 34.505454 <sup>0</sup> E 69.243245 <sup>0</sup>	Bottled	The water was bottled and sealed by COCACOLA company of Afghanistan in Kabul
	2-22	KAREZ mineral water	N/A	Bottled	The water was bottled and sealed by KAREZ mineral water company in Kabul
	2-23	PANJSHER mineral water	N 35.391625 <sup>0</sup> E 69.581838 <sup>0</sup>	Bottled	The water was bottled and sealed by PANJSHER mineral water company in Kabul
	3-1	Khair khana, Kabul	N 34.576339 <sup>0</sup> E 69.140793 <sup>0</sup>	Kitchen tap	The water was supplied by fully covered water pump
	3-2	Sheenah 12 <sup>th</sup> dist	N 34.519825 <sup>0</sup> E 69.297907 <sup>0</sup>	Water Pump	Even the well is fully covered but there was still possibility for pollutants to get in
3 <sup>rd</sup> Phase – October 2015	3-3	Alo khail 16 <sup>th</sup> dist	N 34.524920 <sup>0</sup> E 69.284979 <sup>0</sup>	Water Pump	Even the well is fully covered but there was still possibility for pollutants to get in
	3-4	Sheena 12 <sup>th</sup> dist	N 34.520426 <sup>0</sup> E 69.298334 <sup>0</sup>	Water Pump	Even the well is fully covered but there was still possibility for pollutants to get in

3-5	Alo khail 16 <sup>th</sup> dist	N 34.527148 <sup>0</sup> E 69.280599 <sup>0</sup>	Hand pump	Even the well is fully covered but there was still possibility for pollutants to get in
3-6	Deh Khudaidad 16 <sup>th</sup> dist	N 34.534295 <sup>0</sup> E 69.217324 <sup>0</sup>	Hand pump	The pump and the well is partly covered and there is possibility for pollutants to get in
3-7	Qala Charkhi 8 <sup>th</sup> dist	N 34.519891 <sup>0</sup> E 69.337811 <sup>0</sup>	Hand pump	The pump and the well is partly covered and there is possibility for pollutants to get in
3-8	Chah Habib 8 <sup>th</sup> dist	N 34.519079 <sup>0</sup> E 69.316965 <sup>0</sup>	Hand pump	The pump and the well is partly covered and there is possibility for pollutants to get in
3-9	Chenar Ha 8 <sup>th</sup> dist	N 34.516998 <sup>0</sup> E 69.316242 <sup>0</sup>	Hand pump	The pump and the well is partly covered and there is possibility for pollutants to get in
3-10	Naw abad 16 <sup>th</sup> dist	N 34.545051 <sup>0</sup> E 69.223995 <sup>0</sup>	Hand pump	The pump and the well is partly covered and there is possibility for pollutants to get in
3-11	Qala Zaman 16 <sup>th</sup> dist	N 34.527982 <sup>0</sup> E 69.222232 <sup>0</sup>	Water Pump	Even the well is fully covered but there was still possibility for pollutants to get in
3-12	Masjeed Kareez	N 34.631732 <sup>0</sup> E 69.047479 <sup>0</sup>	Open Spring	The spring is totally open and pollutants can easily get in, buckets are used to get water

3-13	Milad House Kareez	N 34.631399 <sup>0</sup> E 69.047044 <sup>0</sup>	Open Spring	The spring is totally open and pollutants can easily get in, buckets are used to get water
3-14	Wahid kor 16 <sup>th</sup> dist	N 34.529007 <sup>0</sup> E 69.217668 <sup>0</sup>	Open well	The well is totally open and pollutants can easily get in, buckets are used to get water
3-15	Kaka kor 16 <sup>th</sup> dist	N 34.529060 <sup>0</sup> E 69.219121 <sup>0</sup>	Open well	The well is totally open and pollutants can easily get in, buckets are used to get water
3-16	Wahid Hamsiah 16 <sup>th</sup> dist	N 34.529537 <sup>0</sup> E 69.218713 <sup>0</sup>	Open well	The well is totally open and pollutants can easily get in, buckets are used to get water
3-17	Kareez Chashma	N 34.633277 <sup>0</sup> E 69.048172 <sup>0</sup>	Open Spring	The spring is totally open and pollutants can easily get in, buckets are used to get water
3-18	Kareez chah	N 34.631552 <sup>0</sup> E 69.047243 <sup>0</sup>	Open well	The well is totally open and pollutants can easily get in, buckets are used to get water
3-19	Kareez Chah 2	N 34.631463 <sup>0</sup> E 69.047855 <sup>0</sup>	Open well	The well is totally open and pollutants can easily get in, buckets are used to get water
3-20	Khair Khana Nal	N 34.576339 <sup>0</sup> E 69.140793 <sup>0</sup>	Water Pump	Even the well is fully covered but there was still possibility for pollutants to get in

	1-2	Khair Khana Ashpazkhana	N 34.576339 <sup>0</sup> E 69.140793 <sup>0</sup>	Water Pump	Even the well is fully covered but there was still possibility for pollutants to get in

**Table 2**

Table.3 shows results of the  $\mu$ -XRF analyses where all mean values of three spot measurements per sample are given in wt% with standard deviation. Elements that were quantified as zero for all three measurement positions are marked as n.d. (not detected) and the notion F and S stands for phase and sample number, respectively. F1S5 is the only soil sample in the entire sample sets.

	F1S1	F1S2	F1S3	F1S4	F1S5	F2S1	F2S2	F2S3	F2S4	F2S5	F2S1	F3S2	F3S3	F3S4	F3S5
<b>Na K</b>	6.16 ± 0.76	3.85 ± 0.82	1.17 ± 2.03	n.d.	5.41 ± 0.93	6.17 ± 1.92	4.26 ± 0.30	5.27 ± 1.04	n.d.	5.34 ± 0.51	2.50 ± 0.77	3.54 ± 1.67	3.90 ± 0.35	5.78 ± 1.71	2.72 ± 1.56
<b>AlK</b>	15.65 ± 0.28	11.67 ± 1.22	4.10 ± 3.60	n.d.	14.92 ± 1.06	8.43 ± 2.80	6.85 ± 0.70	16.43 ± 0.87	1.45 ± 0.90	15.44 ± 0.35	8.81 ± 5.30	10.30 ± 0.82	9.08 ± 2.41	9.49 ± 2.91	12.03 ± 0.56
<b>SiK</b>	65.83 ± 0.94	43.46 ± 5.77	51.82 ± 26.03	28.29 ± 5.15	65.18 ± 0.32	75.01 ± 3.92	76.60 ± 0.94	65.01 ± 1.50	36.41 ± 7.71	63.37 ± 2.30	73.70 ± 10.25	70.58 ± 2.02	72.65 ± 3.56	74.55 ± 0.61	63.71 ± 11.32
<b>P K</b>	n.d.	n.d.	9.76 ± 6.75	21.88 ± 2.02	n.d.	n.d.	n.d.	n.d.	18.77 ± 1.91	n.d.	12.69 ± 6.85	8.71 ± 4.16	8.84 ± 1.25	4.91 ± 3.18	6.93 ± 5.18
<b>PdL</b>	0.77 ± 1.33	2.90 ± 2.06	n.d.	n.d.	n.d.	5.63 ± 3.88	6.20 ± 1.25	2.78 ± 1.02	n.d.	2.19 ± 1.55	0.39 ± 0.39	1.26 ± 1.08	1.41 ± 0.61	2.80 ± 1.08	5.41 ± 8.46
<b>K K</b>	2.88 ± 0.46	1.86 ± 1.18	0.04 ± 0.07	n.d.	2.59 ± 0.98	0.91 ± 0.50	0.33 ± 0.36	5.01 ± 0.54	9.10 ± 1.11	6.07 ± 1.45	0.06 ± 0.06	0.35 ± 0.14	0.28 ± 0.07	0.55 ± 0.82	0.70 ± 1.05
<b>Ca K</b>	5.98 ± 0.96	27.22 ± 7.49	7.78 ± 3.88	8.64 ± 1.75	6.40 ± 2.30	0.09 ± 0.11	0.05 ± 0.03	0.10 ± 0.01	n.d.	0.30 ± 0.52	0.05 ± 0.06	0.12 ± 0.06	0.10 ± 0.02	0.05 ± 0.04	0.17 ± 0.08
<b>TiK</b>	0.09 ± 0.02	0.46 ± 0.77	n.d.	n.d.	0.15 ± 0.01	0.13 ± 0.02	0.29 ± 0.09	0.25 ± 0.05	n.d.	0.22 ± 0.04	0.22 ± 0.11	2.07 ± 1.65	0.98 ± 0.05	0.84 ± 0.48	4.22 ± 5.68
<b>Mn K</b>	0.05 ± 0.04	0.14 ± 0.06	n.d.	n.d.	0.14 ± 0.12	0.65 ± 0.15	0.59 ± 0.21	0.99 ± 0.19	4.13 ± 1.24	1.80 ± 1.33	1.42 ± 0.92	2.94 ± 0.49	2.67 ± 0.32	1.23 ± 0.92	2.48 ± 1.41
<b>FeK</b>	0.95 ± 0.26	3.05 ± 2.66	6.12 ± 3.59	3.47 ± 0.58	1.44 ± 0.36	2.95 ± 0.32	4.76 ± 0.90	3.77 ± 0.44	1.84 ± 0.96	3.39 ± 0.76	n.d.	0.10 ± 0.11	0.05 ± 0.03	0.02 ± 0.03	0.00 ± 0.01
<b>Cu K</b>	1.51 ± 1.31	3.41 ± 0.66	0.95 ± 0.18	0.45 ± 0.31	3.69 ± 0.61	0.03 ± 0.01	0.07 ± 0.02	0.03 ± 0.03	n.d.	n.d.	n.d.	n.d.	n.d.	n.d.	0.78 ± 1.35
<b>Cr K</b>	0.03 ± 0.01	n.d.	n.d.	n.d.	0.06 ± 0.02	n.d.	n.d.	0.35 ± 0.60	2.63 ± 1.39	n.d.	n.d.	n.d.	n.d.	0.03 ± 0.05	0.59 ± 1.03
<b>ThL</b>	n.d.	0.29 ± 0.50	1.12 ± 0.54	4.89 ± 2.20	n.d.	n.d.	n.d.	n.d.	12.38 ± 3.05	1.45 ± 0.17	n.d.	n.d.	n.d.	n.d.	n.d.
<b>CeL</b>	n.d.	1.51 ± 1.37	8.18 ± 5.83	16.15 ± 2.51	n.d.	n.d.	n.d.	n.d.	5.60 ± 1.50	0.36 ± 0.36	n.d.	n.d.	n.d.	n.d.	n.d.
<b>LaL</b>	n.d.	0.12 ± 0.21	3.20 ± 2.23	7.44 ± 0.97	n.d.	n.d.	n.d.	n.d.	1.09 ± 0.19	0.15 ± 0.10	n.d.	n.d.	n.d.	n.d.	n.d.
<b>S K</b>	n.d.	0.08 ± 0.14	3.63 ± 4.98	1.85 ± 0.86	0.00 ± 0.01	n.d.	n.d.	n.d.	6.57 ± 1.12	n.d.	n.d.	0.00 ± 0.01	0.03 ± 0.06	n.d.	n.d.
<b>AgL</b>	n.d.	n.d.	4.28 ± 2.69	6.87 ± 0.40	n.d.	n.d.	n.d.	n.d.	6.57 ± 1.12	n.d.	n.d.	n.d.	n.d.	n.d.	n.d.
<b>PtL</b>	n.d.	n.d.	0.23 ± 0.25	n.d.	n.d.	n.d.	n.d.	n.d.	n.d.	n.d.	n.d.	n.d.	n.d.	n.d.	n.d.
<b>Hg L</b>	n.d.	n.d.	0.19 ± 0.33	n.d.	n.d.	n.d.	n.d.	n.d.	n.d.	n.d.	n.d.	n.d.	n.d.	n.d.	n.d.
<b>NiK</b>	n.d.	n.d.	0.04 ± 0.07	n.d.	n.d.	n.d.	n.d.	n.d.	n.d.	n.d.	n.d.	n.d.	n.d.	n.d.	n.d.
<b>AsK</b>	n.d.	n.d.	n.d.	0.05 ± 0.08	n.d.	n.d.	n.d.	n.d.	0.03 ± 0.06	n.d.	n.d.	n.d.	n.d.	n.d.	n.d.
<b>SeK</b>	n.d.	n.d.	n.d.	n.d.	n.d.	n.d.	n.d.	n.d.	n.d.	n.d.	0.05 ± 0.09	n.d.	n.d.	n.d.	n.d.
<b>BaL</b>	n.d.	n.d.	n.d.	n.d.	n.d.	n.d.	n.d.	n.d.	n.d.	n.d.	0.15 ± 0.26	n.d.	n.d.	0.01 ± 0.02	0.08 ± 0.14
<b>W L</b>	n.d.	n.d.	n.d.	n.d.	n.d.	n.d.	n.d.	n.d.	n.d.	n.d.	n.d.	n.d.	n.d.	0.24 ± 0.14	n.d.



Nd L	n.d.	n.d.	n.d.	n.d.	n.d.	n.d.	n.d.	n.d.	n.d.	n.d.	n.d.	n.d.	n.d.	n.d.	0.18 ± 0.32
---------	------	------	------	------	------	------	------	------	------	------	------	------	------	------	----------------

**Table 3**

**Table 4** the chemical parameters proposed by AUWSSC

Essential Chemical Parameters for AUWSSC				
Properties/Parameters	Standard values for Afghanistan [mg/Liter = ppm = mg/kg] - Maximum Permissible	WHO Guidelines as in 2011 [mg/Liter = ppm = mg/kg]	National Standard of most Asian countries [mg/Liter = ppm = mg/kg]	General Remarks
Aluminium (Al)	0.2	N/A	0.2	
Antimony (Sb)	0.02	0.02	0.02	
Barium (Ba)	0.7	0.7	0.7	
Boron (B)	2.4	2.4	2.4	
Cadmium (Cd)	0.003	0.003	0.003	
Chlorine (Cl)	250	N/A	250	Permissible limit in the absence of alternate water

				source can rise up to 1000mg/l.
Chromium (Cr)	0.05	0.05	0.05	
Copper (Cu)	2	2	2	
Iron (Fe)	0.3	N/A	0.3	
Sodium (Na)	200	N/A	200	
Sulfate ( SO <sub>2</sub> -4)	250	N/A	250	Permissible limit in the absence of alternate water source can rise up to 400mg/l.
Magnesium (Mg)	30	N/A	30	Permissible limit in the absence of alternate water source can rise up to 100mg/l.
Calcium(Ca)	75	N/A	75	Permissible limit in the absence of alternate water source can rise up to 200mg/l.
Cobalt (Co)				
Mercury (Hg)				

Toxic Chemical Parameters				
Cyanide (Cn)	0.05	N/A	0.05	
Arsenic (As)	0.05	0.01	0.01-0.05	
Fluorine (F)	1.5	1.5	1.5	
Lead (Pb)	0.01	0.01	0.01	
Manganese (Mn)	0.3	N/A	0.3	
Nickel (Ni)	0.07	0.07	0.07	
Nitrate (NO <sub>3</sub> )	50	50	50	
Nitrite (NO <sub>2</sub> )	3	3	3	
Nitrate as Nitrogen	11	11	11	
Selenium (Se)	0.04	0.04	0.04	
Zinc (Zn)	3	N/A	3	

**Table 4**

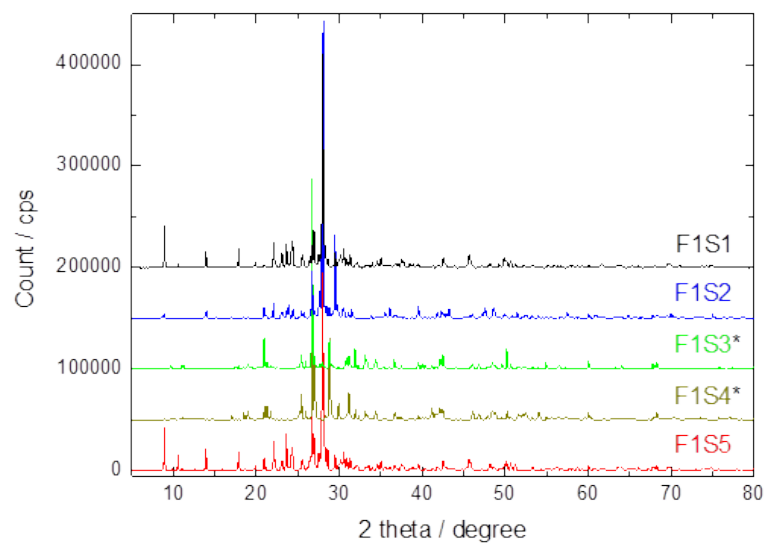


Figure1. Powder X-ray diffractograms for five samples of the F1 series. X-ray source: Cu K $\alpha$  radiation. XRF detected a significant amount of thorium in these samples.

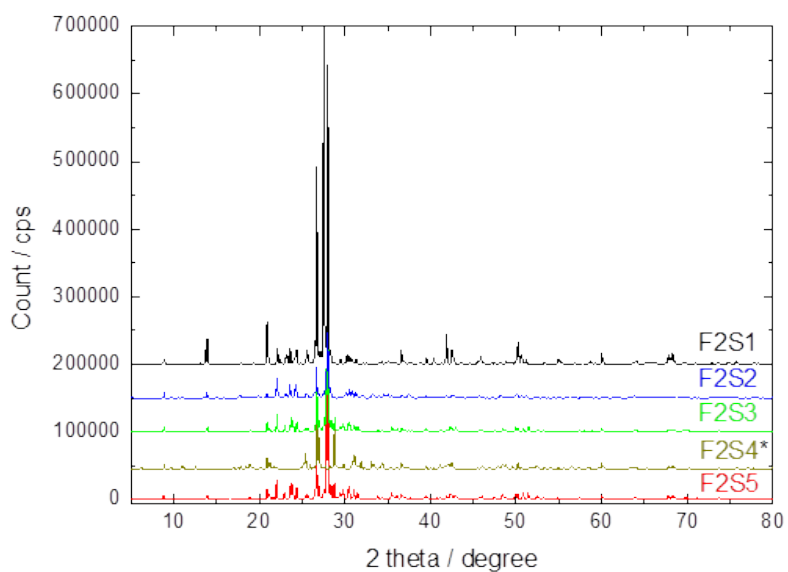


Figure2. Powder X-ray diffractograms for five samples of the F2 series. X-ray source: Cu K $\alpha$  radiation. XRF detected a significant amount of thorium in this sample.

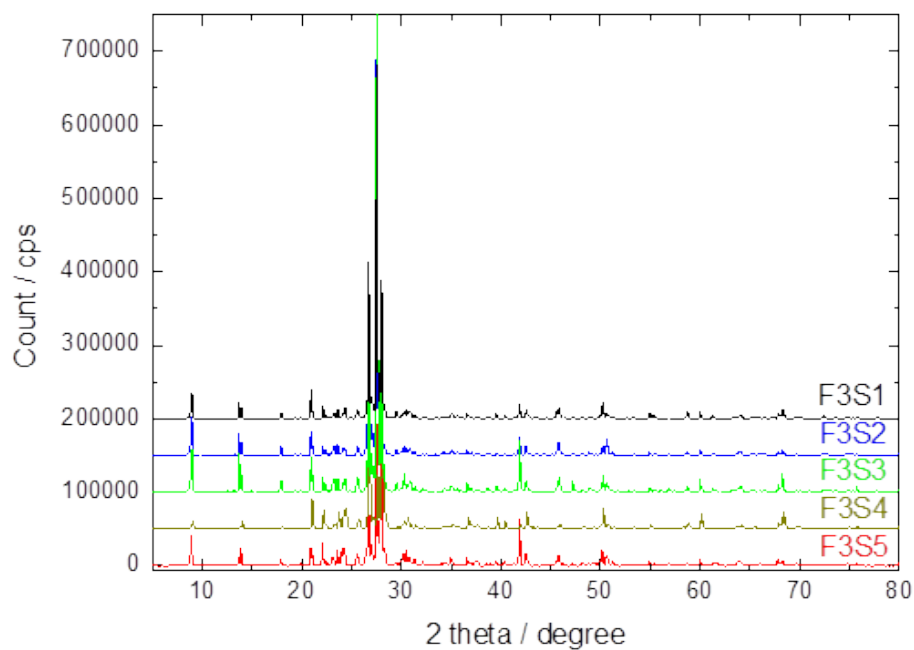


Figure3. Powder X-ray diffractograms for five samples of the F3 series. X-ray source: Cu K $\alpha$  radiation.

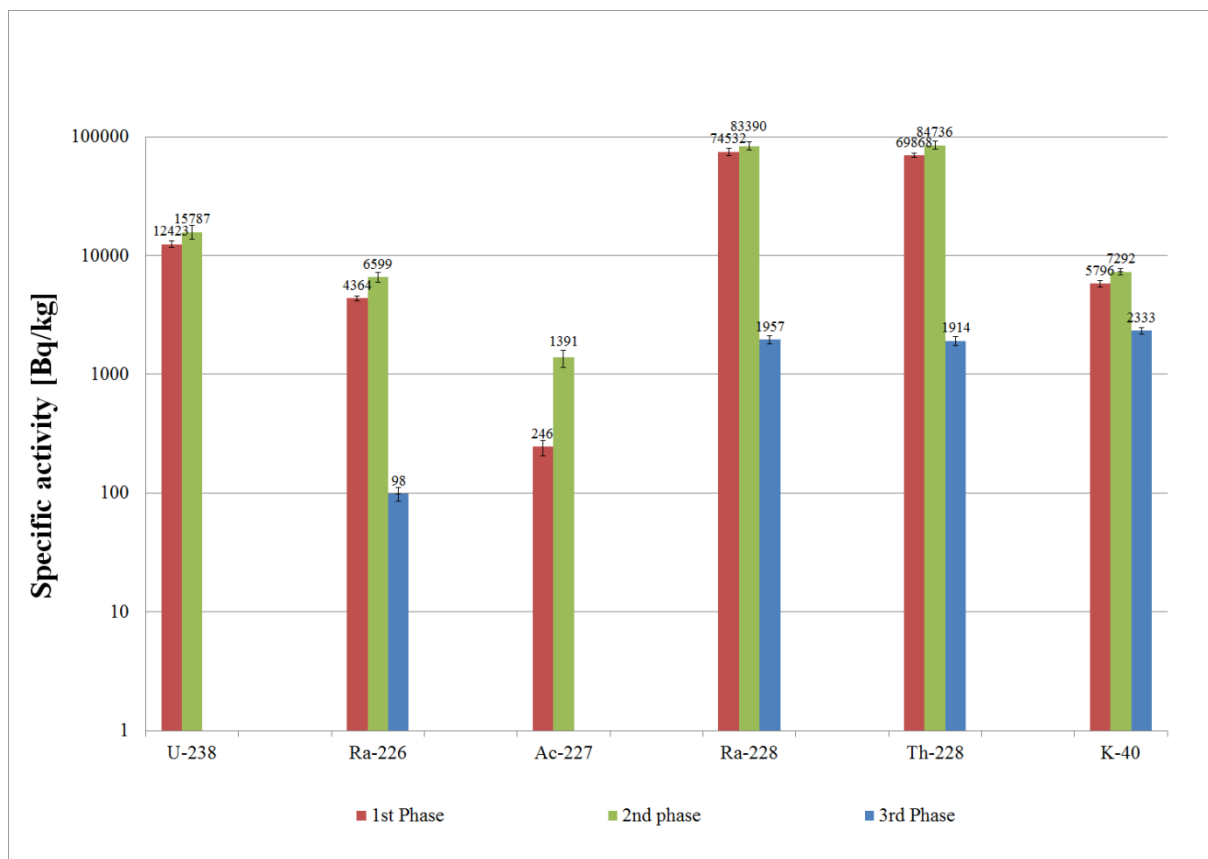


Fig.4 Activity concentration of different isotopes of the uranium, actinium and thorium series. , where isotopes are shown on the x-axis and the y-axis shows the activity in a logarithmic scale.